



RESEARCH LETTER

10.1002/2014GL061475

Key Points:

- We study flow and transport in 3-D porous media at the pore scale
- Longitudinal spreading is superdiffusive; transverse spreading is subdiffusive
- Anomalous behavior originates from the intermittent structure of the velocity

Correspondence to:

R. Juanes,
juanes@mit.edu

Citation:

Kang, P. K., P. de Anna, J. P. Nunes, B. Bijeljic, M. J. Blunt, and R. Juanes (2014), Pore-scale intermittent velocity structure underpinning anomalous transport through 3-D porous media, *Geophys. Res. Lett.*, 41, 6184–6190, doi:10.1002/2014GL061475.

Received 11 AUG 2014

Accepted 25 AUG 2014

Accepted article online 27 AUG 2014

Published online 15 SEP 2014

Pore-scale intermittent velocity structure underpinning anomalous transport through 3-D porous media

Peter K. Kang¹, Pietro de Anna¹, Joao P. Nunes^{2,3}, Branko Bijeljic², Martin J. Blunt², and Ruben Juanes¹

¹Department of Civil and Environmental Engineering, Massachusetts Institute of Technology, Cambridge, Massachusetts, USA, ²Department of Earth Science and Engineering, Imperial College London, London, UK, ³Petrobras E&P, Rio de Janeiro, Brazil

Abstract We study the nature of non-Fickian particle transport in 3-D porous media by simulating fluid flow in the intricate pore space of real rock. We solve the full Navier-Stokes equations at the same resolution as the 3-D micro-CT (computed tomography) image of the rock sample and simulate particle transport along the streamlines of the velocity field. We find that transport at the pore scale is markedly anomalous: longitudinal spreading is superdiffusive, while transverse spreading is subdiffusive. We demonstrate that this anomalous behavior originates from the intermittent structure of the velocity field at the pore scale, which in turn emanates from the interplay between velocity heterogeneity and velocity correlation. Finally, we propose a continuous time random walk model that honors this intermittent structure at the pore scale and captures the anomalous 3-D transport behavior at the macroscale.

1. Introduction

Fluid flow and transport in geologic porous media is critical to many natural and engineered processes, including sustainable exploitation of groundwater resources [Harvey *et al.*, 2002; Gleeson *et al.*, 2012], enhanced oil recovery [Orr and Taber, 1984], geologic carbon sequestration [IPCC, 2005; Szulczewski *et al.*, 2012], geologic nuclear waste disposal [Yoshida and Takahashi, 2012], and water filtration [Elliott *et al.*, 2008].

Despite the broad relevance of flow and transport through geologic porous media, our understanding still faces significant challenges. One such challenge is the almost ubiquitous observation of anomalous (non-Fickian) transport behavior from laboratory experiments in packed beds [Kandhai *et al.*, 2002; Moroni *et al.*, 2007], sand columns [Cortis and Berkowitz, 2004], and rock samples [Scheven *et al.*, 2005; Bijeljic *et al.*, 2011] to field-scale experiments [Garabedian *et al.*, 1991; Le Borgne and Gouze, 2008]. The signatures of anomalous behavior are early breakthrough, long tailing of the first passage time distribution, non-Gaussian or multipeaked plume shapes, and nonlinear scaling of the mean square displacement—effects that cannot be captured by a traditional advection-dispersion formulation. There are several models that describe and predict non-Fickian transport, by replicating the broad (power law) distribution of velocity; these include multirate mass transfer [Haggerty and Gorelick, 1995], fractional advection-dispersion [Benson *et al.*, 2001], and continuous time random walk (CTRW) models [Berkowitz *et al.*, 2006; Bijeljic and Blunt, 2006], and the equivalence between the models has been shown for certain cases [Dentz and Berkowitz, 2003].

In addition to velocity heterogeneity, recent studies have pointed out the importance of velocity correlation in the signature of anomalous transport, and have incorporated velocity correlation in various forms [Le Borgne *et al.*, 2008; Dentz and Bolster, 2010; Kang *et al.*, 2011; Ederly *et al.*, 2014]. In particular, numerical simulations using smoothed particle hydrodynamics of flow and transport on simple 2-D porous media suggest that longitudinal spreading is strongly modulated by the intermittent structure of Lagrangian velocity [de Anna *et al.*, 2013], which is also observed in laboratory experiments in 3-D glass bead packs [Datta *et al.*, 2013]. However, the role of velocity correlation on anomalous transport has not yet been studied for real 3-D rocks, and flow fields through 3-D-disordered porous media are fundamentally different from flow fields in 2-D or 3-D ordered porous media.

Moreover, a fundamental question remains: how does the heterogeneous and correlated structure of Lagrangian velocity impact *transverse spreading*? It is known that transverse spreading largely controls overall mixing and, as a result, many chemical and biological processes in natural systems [Bijeljic and Blunt, 2007; Tartakovsky *et al.*, 2008; Willingham *et al.*, 2008; Tartakovsky, 2010; Rolle *et al.*, 2012]. In this Letter, we study flow and particle transport through porous rock (Berea sandstone), imaged at the pore scale with X-ray

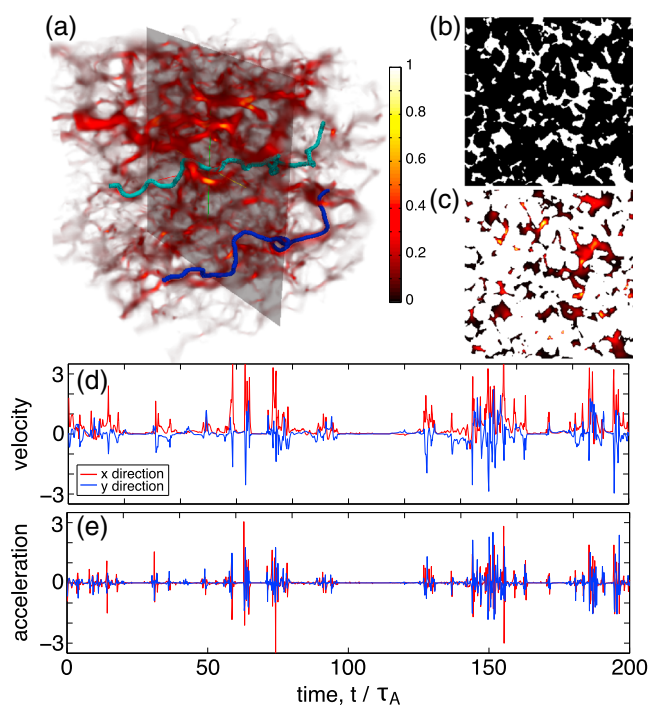


Figure 1. (a) Three-dimensional Eulerian velocity magnitude ($|\mathbf{v}|$) through a Berea sandstone sample of size 1.66 mm (approximately 8 pore lengths) on each side. The velocity magnitude is normalized with respect to the maximum velocity, as indicated by the color bar; blue and cyan solid lines indicate two particle trajectories. The domain is discretized into 300^3 voxels with resolution $5.55 \mu\text{m}$ (approximately 0.03 pore lengths). (b) Cross section of the Berea sandstone at rescaled distance $\xi_x = \frac{x}{\lambda_c} = 4.16$, showing the pore space (white) and solid grains (black). The average porosity (fraction of void space in the sample) is approximately 18.25%. (c) Cross section of the velocity magnitude at rescaled distance $\xi_x = 4.16$ (warm colors correspond to higher velocities), illustrating the presence of preferential flow paths. (d and e) Time series of the normalized Lagrangian velocity and acceleration, respectively, for the blue particle trajectory in Figure 1a. The Lagrangian statistics exhibit strongly intermittent behavior in both longitudinal and transverse directions.

To obtain the flow field, we solve the full Navier-Stokes equations through the pore geometry of the Berea sandstone with no-slip boundary conditions at the grain surfaces, using a finite volume method [OpenFOAM, 2011; Bijeljic *et al.*, 2013]. We impose constant pressure boundary conditions at the inlet and outlet faces. The Eulerian velocity field \mathbf{v} exhibits a complex structure with multiple preferential flow channels and stagnation zones (Figure 1a).

To study the transport properties, we simulate the advection of particles along streamlines of the stationary 3-D flow field. We trace streamlines using a semianalytical formulation to compute entry and exit positions, and transit times, through each voxel traversed by individual streamlines [Mostaghimi *et al.*, 2012]. To initialize the streamlines, we place 10^4 particles at the inlet face, following a flux-weighted spatial distribution through the pore geometry. To obtain particle trajectories that are long enough to observe macroscopic behavior, we concatenate particle trajectories randomly within the same class of the flux probability distribution (we have confirmed that the flux distribution at inlet and outlet faces are virtually identical). To avoid boundary effects on transverse displacement, we reinject a particle (following the same flux-weighted protocol) whenever its distance to one of the lateral boundaries is less than $11.1 \mu\text{m}$ (2 voxels). We compute the mean Lagrangian velocity across all trajectories, \bar{v} , and define the characteristic time to travel the average pore size as $\tau_A = \lambda_c / \bar{v}$, which is used to rescale time.

microtomography (micro-CT imaging). We observe strongly non-Fickian spreading behavior in both longitudinal and transverse directions and find complementary anomalous behavior: longitudinal spreading is superdiffusive, while transverse spreading is subdiffusive. We show that the interplay between pore-scale velocity correlation and velocity heterogeneity is responsible for the observed anomalous behavior. We then develop an effective stochastic transport model for 3-D porous media that incorporates the microscale velocity structure in the form of a continuous time random walk (CTRW) with one-step correlation.

2. Fluid Flow and Particle Tracking Through Berea Sandstone

We analyze the 3-D Lagrangian velocities of a Newtonian fluid flowing through a cubic sample of Berea sandstone of size $L = 1.66 \text{ mm}$ on each side. Micro-CT is used to obtain the 3-D image of the porous structure at a resolution of $5.55 \mu\text{m}$ (the image size is 300^3 voxels). Image segmentation identifies each voxel as either solid or void. The characteristic length of the mean pore size is $\lambda_c \approx 200 \mu\text{m}$ [Mostaghimi *et al.*, 2012], which is used to define the nondimensional distance $\xi_x = x / \lambda_c$ (the sample has ~ 8 characteristic pore lengths in each direction).

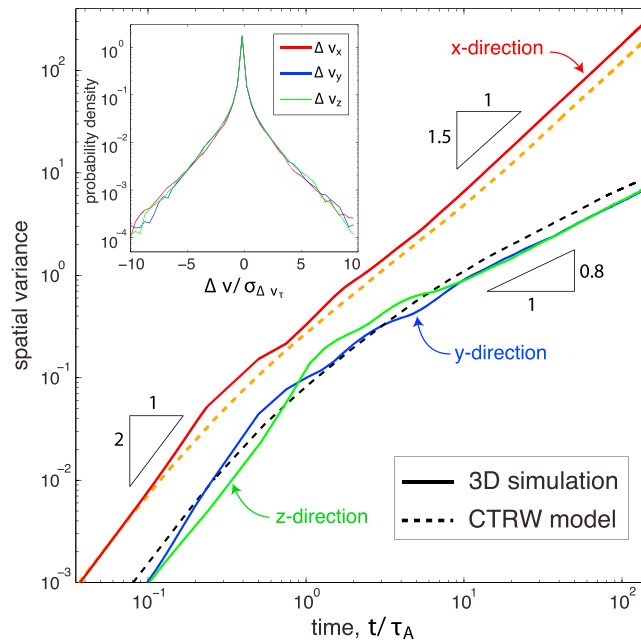


Figure 2. Time evolution of the centered second spatial moments from particle-tracking simulation (solid line) and the prediction with correlated CTRW (dashed line). In the x direction, particle dispersion is superdiffusive with slope ~ 1.5 , and in the y and z directions, dispersion is subdiffusive with slope ~ 0.8 . Inset: Probability density distributions of the normalized Lagrangian velocity increments in x , y , and z directions for a time lag $\tau = \tau_A/4$. Velocity increments are normalized with respect to their standard deviation $\sigma_{\Delta v_i}$.

as *intermittency*. Flow intermittency is a well known phenomenon in turbulent flows, where it is quantified by the properties of the structure functions [Pope, 2000]. Even though the flow in our system is laminar, our simulations show that the geometry of real 3-D rock also leads to strongly intermittent behavior. Similar intermittent behavior in the longitudinal direction has been observed in a 2-D porous medium consisting of a random distribution of disks [de Anna et al., 2013]. In the transverse direction, particles with high positive velocities jump to high negative velocities—an anticorrelation that was also observed in the particle transport through simple lattice networks [Kang et al., 2011].

3. Non-Fickian Spreading and Intermittency

To investigate the impact of the observed intermittent behavior of individual particles on the macroscopic spreading of the ensemble of particles, we compute the time evolution of the longitudinal and transverse mean square displacements (MSD) with respect to the center of mass of a point injection, i.e., initializing every particle's starting position to an identical reference point. For the longitudinal direction (x), the MSD is given by $\sigma_x^2(t) = \langle (x(t) - \langle x(t) \rangle)^2 \rangle$ where $\langle \cdot \rangle$ denotes the average over all particles. The same definition is applied to the transverse directions to compute σ_y^2 and σ_z^2 . At early times, longitudinal MSD exhibits ballistic scaling, $\sigma_x^2 \sim t^2$, characteristic of perfectly correlated stratified flows [Taylor, 1921]. After this initial period, the MSD follows a non-Fickian *superdiffusive* scaling $\sigma_x^2(t) \sim t^{1.5}$. The MSD in the transverse directions also scales as $\sigma_y^2, \sigma_z^2 \sim t^2$ at early times but, in contrast, then slows down to an asymptotic non-Fickian *subdiffusive* scaling $\sigma_y^2, \sigma_z^2 \sim t^{0.8}$ (Figure 2). The non-Fickian scaling is persistent over 100 characteristic times (τ_A). Such persistent non-Fickian scaling is partly due to the infinite Peclet number in our system. As we introduce diffusion, the transition to Fickian scaling would occur earlier [Berkowitz et al., 2006; Bolster et al., 2014]. Vortices created by inertia can also lead to anomalous transport [Cardenas, 2008]. In our system, however, the Reynolds number is in the order of 10^{-3} , and we have confirmed that inertia is not strong enough to create eddies.

The rock sample used for the determination of the underlying flow field is approximately 8 pore lengths on each side. However, solute transport is simulated over *many hundreds of pores* by the use of a Lagrangian particle transport method and reinjection of particles. This is equivalent to studying macroscale transport properties where the medium heterogeneity is restricted to approximately 8^3 pores, but a much larger system size. Berea sandstone, the rock we use in our study, is relatively homogeneous, and this pore structure results in a smooth flow field. Therefore, we believe that our rock sample of Berea sandstone is representative for single-phase flow and transport.

In Figure 1a we plot two particle trajectories. The temporal evolution of the Lagrangian velocity and acceleration for a particle exhibits two alternating states: long periods of stagnation and bursts of high variability (Figures 1d and 1e), both in the longitudinal (x) and transverse (y, z) directions of the flow. This irregular pattern of alternating states is known

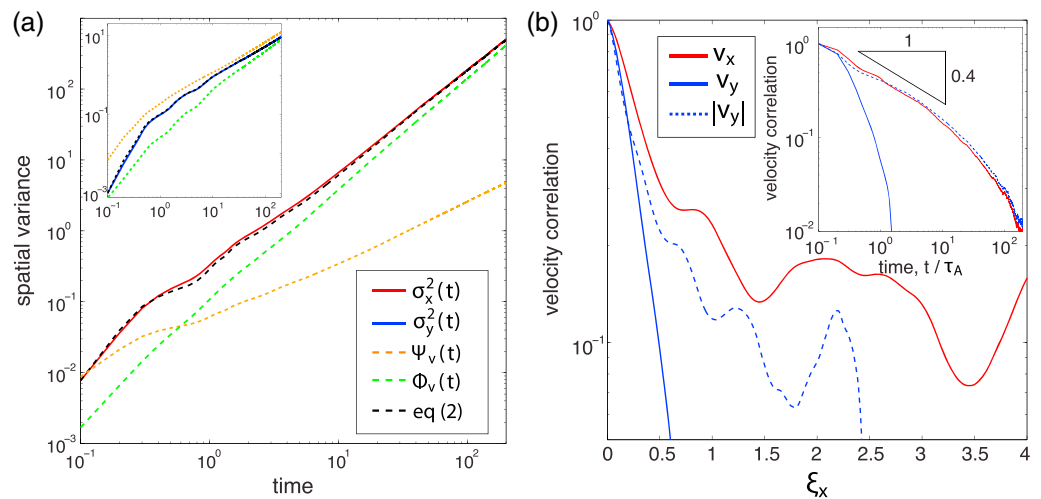


Figure 3. (a) Time evolution of the centered second spatial moments in the *longitudinal* direction from particle tracking simulation (red solid line), approximation from equation (2) (black dashed line), and estimations from velocity heterogeneity alone ($\Psi_v(t)$, orange dashed line) and velocity correlation alone ($\Phi_v(t)$, green dashed line). The orange and green lines are shifted along the y axis for clarity. Inset: Time evolution of the centered second spatial moments in the *transverse* direction. (b) Longitudinal (x , red) and transverse (y , blue) Lagrangian velocity autocorrelation as a function of *space* along the longitudinal direction. All functions are short-ranged. Inset: Longitudinal (red) and transverse (blue) Lagrangian velocity autocorrelation as a function of *time*. Note the strong, long range, correlation of the longitudinal velocity v_x and the absolute value of the transverse velocity, $|v_y|$.

We study the role of the intermittent velocity structure on the observed multidimensional anomalous spreading in real 3-D rock. To quantify the intermittent behavior, we compute the velocity increment probability density function (PDF). The Lagrangian velocity increment associated to a time lag τ is defined as $\Delta_\tau v = v(t + \tau) - v(t)$ where $v(t) = [x(t + \tau) - x(t)]/\tau$. The velocity increments are rescaled with respect to their standard deviation, $\Delta_\tau v / \sigma_{\Delta_\tau v}$. We find that the velocity increment PDFs in both the longitudinal and transverse directions collapse (Figure 2, inset), an indication that intermittent behavior is equally significant in all directions. This multidimensional intermittency originates from the combined effect of the 3-D pore structure and the divergence-free constraint on the velocity field, which results in a misalignment between the local velocity and the mean flow direction. The PDF of the velocity increments is characterized by a sharp peak near zero and exponential tails. The peak reflects the trapping of particles in stagnation zones, while the exponential tails indicate that large velocity jumps are also probable due to the strong heterogeneity in the velocity field—a signature of the observed intermittency [de Anna et al., 2013; Datta et al., 2013]. The non-Gaussian character of the velocity increment PDF persists at long times (not shown), an indication that pore-scale fluid flow cannot be modeled using the Langevin description with white noise [Tartakovsky, 2010].

4. Lagrangian Velocity Correlation Structure and Origin of Anomalous Transport

Let $\chi_v(\tau, \eta)$ be the velocity autocorrelation between times τ and η

$$\chi_v(\tau, \eta) = \frac{\langle [v(\tau) - \langle v(\tau) \rangle][v(\eta) - \langle v(\eta) \rangle] \rangle}{\sigma_v(\tau)\sigma_v(\eta)}, \quad (1)$$

where $\sigma_v^2(\eta)$ is the variance of the Lagrangian velocity at time η . Owing to its definition, the MSD can be expressed as $\sigma_x^2(t) = 2 \int_0^t d\eta \sigma_v(\eta) \int_0^\eta d\tau \sigma_v(\tau) \chi_v(\tau, \eta)$ [Bear, 1972]. We have confirmed that the velocity standard deviation σ_v decays in time much more slowly than the velocity autocorrelation χ_v . In this case, the MSD can be approximated as

$$\sigma_x^2(t) \approx 2 \int_0^t d\eta \sigma_v^2(\eta) \int_0^\eta d\tau \chi_v(\tau, \eta). \quad (2)$$

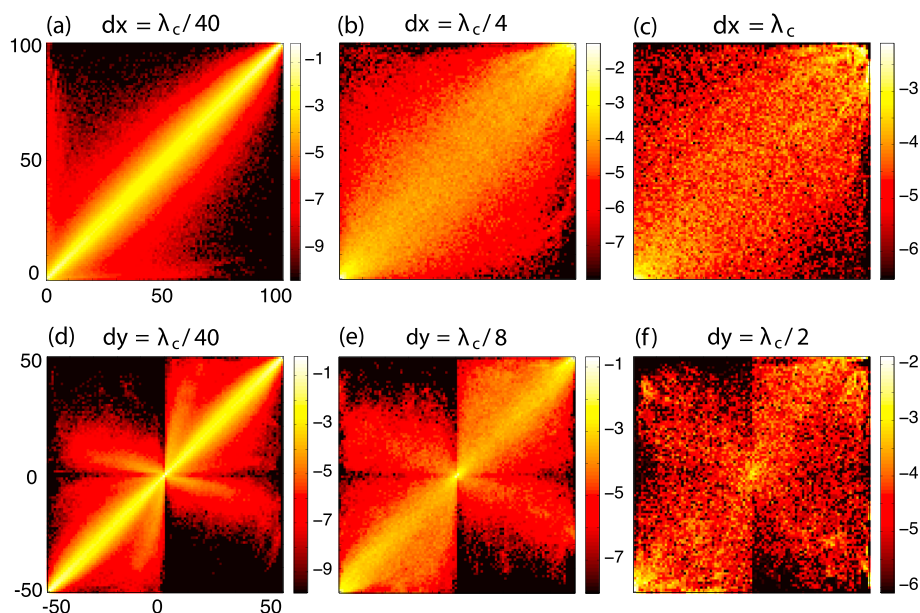


Figure 4. (a–c) Longitudinal (x) transition matrix with $N = 100$ velocity classes for different values of the space transition $\Delta x/\lambda_c$. The velocity correlation decreases as the sampling distance Δx increases. (d–f) Transverse (y) transition matrix with $N = 100$ velocity classes for different Δy values. We assign 50 bins for positive velocity and another 50 for negative velocity. The z directional transition matrix is almost identical to y directional transition matrix.

To study the independent roles of velocity heterogeneity and velocity correlation on particle spreading, we define $\Psi_v(t) = \int_0^t d\eta \sigma_v^2(\eta)$ and $\Phi_v(t) = \int_0^t d\eta \int_0^\eta d\tau \chi_v(\tau, \eta)$, respectively. We observe that the anomalous scaling of particle spreading is dominated by velocity correlation (Φ_v) in the longitudinal direction and, in contrast, by velocity heterogeneity (Ψ_v) in the transverse direction (Figure 3a). However, neither velocity correlation nor velocity heterogeneity alone can fully explain the observed anomalous spreading in our system.

To gain insight into the velocity correlation structure, we compute the velocity autocorrelation as a function of *time* and *space* (Figure 3). From our qualitative and quantitative analysis of intermittency in the Lagrangian statistics (Figures 1d and 1e and inset of Figure 2, respectively), it is not surprising that the longitudinal velocity autocorrelation, χ_{v_x} , is slow decaying in time (Figure 3b, inset). Moreover, while the transverse velocity autocorrelation, χ_{v_y} , decays faster in time, this does not mean that it has short-range correlation; indeed, the absolute magnitude of the transverse velocity, $|v_y|$, exhibits long-range temporal autocorrelation (Figure 3b, inset), highlighting the crucial fact that the transverse velocity is mean reverting but strongly correlated in time—a phenomenon also observed in turbulence for velocity increments [Mordant *et al.*, 2002]. This mean-reverting behavior in the transverse direction may lead to subdiffusive transverse spreading, whereas the existence of a mean drift in longitudinal direction may lead to superdiffusive longitudinal spreading [Dentz *et al.*, 2004].

The Lagrangian correlation structure is drastically different as a function of space, instead of time—a key insight first pointed out in *Le Borgne et al.* [2008] for Darcy flow in heterogeneous media. The longitudinal and transverse velocity autocorrelation, as a function of space ξ_x , are all short ranged and decay exponentially (Figure 3b).

5. Continuous Time Random Walk Model

The exponential decay of autocorrelation is characteristic of Markov processes [Risken, 1989], which suggests that the effective pore-scale velocity transitions in space can be captured by a one-step correlated model in space. We propose a correlated CTRW macroscopic model [Le Borgne *et al.*, 2008; Tejedor and Metzler, 2010], where the velocity heterogeneity structure and the one-step velocity correlation are

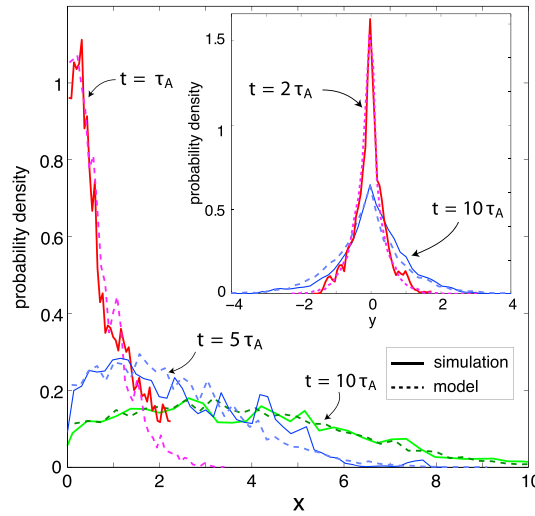


Figure 5. Longitudinal projection of the particle density distribution at fixed times ($t = \tau_A, 5\tau_A,$ and $10\tau_A$) from direct pore-scale simulation (solid line) and the correlated CTRW model prediction (dashed line). Inset: Transverse projection of the particle density distribution at fixed times ($t = 2\tau_A$ and $10\tau_A$) from direct simulation (solid line) and the respective CTRW model prediction (dashed line). Different colors indicate different times.

Figure 4. For the longitudinal direction, the high probabilities along the diagonal of T_1 reflect the strong persistence in the magnitude of longitudinal velocity. For the transverse direction, this effect is also present, but in addition, we observe high probability values along the opposite diagonal, as a result of the transverse velocity anticorrelation due to local flow reversal (Figure 1d).

Average particle motion can be described by the following system of Langevin equations:

$$\zeta_{n+1} = \zeta_n + \Delta\zeta \frac{v_\zeta(n\Delta\zeta)}{|v_\zeta(n\Delta\zeta)|}, \quad t_{n+1} = t_n + \frac{\Delta\zeta}{|v_\zeta(n\Delta\zeta)|}, \quad (4)$$

where $|v_\zeta|$ denotes the absolute value of v_ζ and $\zeta = x, y, z$. We have directionality information in $\frac{v_\zeta(n\Delta\zeta)}{|v_\zeta(n\Delta\zeta)|}$. When $\frac{v_\zeta(n\Delta\zeta)}{|v_\zeta(n\Delta\zeta)|}$ is +1, particles jump forward ($+\Delta\zeta$), and when $\frac{v_\zeta(n\Delta\zeta)}{|v_\zeta(n\Delta\zeta)|}$ is -1, particles jump backward ($-\Delta\zeta$). CTRW simulations are performed independently in each direction with their respective transition matrix, and we choose $\Delta x = \lambda_c/4, \Delta y = \lambda_c/8$ and $\Delta z = \lambda_c/8$, based on the characteristic correlation length of the exponential decay of the spatial velocity autocorrelation (Figure 3a). Note that $\Delta\zeta$ is a physical correlation length scale, which enables capturing the intermittent velocity structure with one-step velocity correlation information. We assume that the sequence of Lagrangian velocities $\{v_\zeta(n\Delta\zeta)\}_{n=0}^\infty$ can be approximated by a Markov process: initial particle velocities are chosen randomly from the initial velocity distribution, and each new velocity at the next time step ($n + 1$) is determined from the velocity at the current time step (n) and the one-step transition matrix T_1 (Figure 4) [Le Borgne et al., 2008; Kang et al., 2011].

The proposed correlated CTRW model accurately predicts the plume evolution in all space directions, as evidenced by the longitudinal and the transverse projections of particle density at fixed times (Figure 5) and by the MSDs in both longitudinal and transverse directions (Figure 2). The model captures nicely the early ballistic regime, the late time scaling, and the transition time, without any fitting parameters. Since the transition matrix is the only input to our model, which is measured directly from the pore-scale information obtained by solving the full Navier-Stokes equations, this validates the proposed CTRW framework. Taken together, our findings point to the critical role of velocity intermittency at the pore scale on particle spreading and, consequently, on mixing and reactive transport processes in porous media flows.

characterized by a velocity transition matrix derived from the pore-scale 3-D simulations [Le Borgne et al., 2008; Kang et al., 2011]. The velocity transition matrix is the only input to our model.

We denote by $r_m(v_\zeta|v'_\zeta)$ the transition probability density to encounter a velocity v_ζ after $n + m$ steps, given that the particle velocity was v'_ζ after n steps (here ζ refers to any of the space directions, x, y, z). To evaluate the discrete transition probability from the simulated 3-D particle trajectories, we discretize the particle velocity distribution into $N = 100$ classes with equiprobable binning, $v_\zeta \in \bigcup_{j=1}^N (v_\zeta^j, v_\zeta^{j+1})$, and define the m -step transition probability matrix:

$$T_m(k|j) = \int_{v_\zeta^k}^{v_\zeta^{k+1}} dv'_\zeta \int_{v_\zeta^j}^{v_\zeta^{j+1}} dv''_\zeta r_m(v_\zeta|v'_\zeta) p(v'_\zeta) / \int_{v_\zeta^j}^{v_\zeta^{j+1}} dv'_\zeta p(v'_\zeta), \quad (3)$$

where $p(v'_\zeta)$ is the univariate velocity distribution. The one-step velocity transition matrix (T_1), in longitudinal and transverse directions, is shown in

Acknowledgment

This work was funded by the US Department of Energy through a DOE CAREER Award (grant DE-SC0003907) and a DOE Mathematical Multi-faceted Integrated Capability Center (grant DE-SC0009286) to R.J. J.P.N. acknowledges funding from Petrobras.

The Editor thanks two anonymous reviewers for their assistance in evaluating this paper.

References

- Bear, J. (1972), *Dynamics of Fluids in Porous Media*, Elsevier, New York.
- Benson, D. A., R. Schumer, M. M. Meerschaert, and S. W. Wheatcraft (2001), Fractional dispersion, Lévy motion, and the MADE tracer tests, *Transp. Porous Media*, *42*, 211–240.
- Berkowitz, B., A. Cortis, M. Dentz, and H. Scher (2006), Modeling non-Fickian transport in geological formations as a continuous time random walk, *Rev. Geophys.*, *44*, RG2003, doi:10.1029/2005RG000178.
- Bijeljic, B., and M. J. Blunt (2006), Pore-scale modeling and continuous time random walk analysis of dispersion in porous media, *Water Resour. Res.*, *42*, W01202, doi:10.1029/2005WR004578.
- Bijeljic, B., and M. J. Blunt (2007), Pore-scale modeling of transverse dispersion in porous media, *Water Resour. Res.*, *43*, W12511, doi:10.1029/2006WR005700.
- Bijeljic, B., P. Mostaghimi, and M. J. Blunt (2011), Signature of non-Fickian solute transport in complex heterogeneous porous media, *Phys. Rev. Lett.*, *107*, 204502.
- Bijeljic, B., A. Raeni, P. Mostaghimi, and M. J. Blunt (2013), Predictions of non-Fickian solute transport in different classes of porous media using direct simulation on pore-scale images, *Phys. Rev. E*, *87*, 013011.
- Bolster, D., Y. Méheust, T. Le Borgne, J. Bouquain, and P. Davy (2014), Modeling preasymptotic transport in flows with significant inertial and trapping effects—The importance of velocity correlations and a spatial Markov model, *Adv. Water Res.*, *70*, 89–103.
- Cardenas, M. B. (2008), Three-dimensional vortices in single pores and their effects on transport, *Geophys. Res. Lett.*, *35*, L18402, doi:10.1029/2008GL035343.
- Cortis, A., and B. Berkowitz (2004), Anomalous transport in “classical” soil and sand columns, *Soil Sci. Soc. Am. J.*, 1539–1548.
- Datta, S. S., H. Chiang, T. S. Ramakrishnan, and D. A. Weitz (2013), Spatial fluctuations of fluid velocities in flow through a three-dimensional porous medium, *Phys. Rev. Lett.*, *111*, 064501.
- de Anna, P., T. Le Borgne, M. Dentz, A. M. Tartakovsky, D. Bolster, and P. Davy (2013), Flow intermittency, dispersion, and correlated continuous time random walks in porous media, *Phys. Rev. Lett.*, *110*, 184502.
- Dentz, M., and B. Berkowitz (2003), Transport behavior of a passive solute in continuous time random walks and multirate mass transfer, *Water Resour. Res.*, *39*(5), 1111, doi:10.1029/2001WR001163.
- Dentz, M., and D. Bolster (2010), Distribution- versus correlation-induced anomalous transport in quenched random velocity fields, *Phys. Rev. Lett.*, *105*, 244301.
- Dentz, M., A. Cortis, H. Scher, and B. Berkowitz (2004), Time behavior of solute transport in heterogeneous media: Transition from anomalous to normal transport, *Adv. Water Res.*, *27*, 155–173.
- Ederly, Y., A. Guadagnini, H. Scher, and B. Berkowitz (2014), Origins of anomalous transport in heterogeneous media: Structural and dynamic controls, *Water Resour. Res.*, *50*, 1490–1505, doi:10.1002/2013WR015111.
- Elliott, M. A., C. E. Stauber, F. Koksai, F. A. DiGianno, and M. D. Sobsey (2008), Reductions of E. coli, echovirus type 12 and bacteriophages in an intermittently operated household-scale slow sand filter, *Water Res.*, *42*(10), 2662–2670.
- Garabedian, S. P., D. R. LeBlanc, L. W. Gelhar, and M. A. Celia (1991), Large-scale natural gradient tracer test in sand and gravel, Cape Cod, Massachusetts 2. Analysis of spatial moments for a nonreactive tracer, *Water Resour. Res.*, *27*(5), 911–924.
- Gleeson, T., Y. Wada, M. F. P. Bierkens, and L. P. H. van Beek (2012), Water balance of global aquifers revealed by groundwater footprint, *Nature*, *488*(7410), 197–200.
- Haggerty, R., and S. M. Gorelick (1995), Multiple-rate mass transfer for modeling diffusion and surface reactions in media with pore-scale heterogeneity, *Water Resour. Res.*, *31*(10), 2383–2400.
- Harvey, C. F., et al. (2002), Arsenic mobility and groundwater extraction in Bangladesh, *Science*, *298*(5598), 1602–1606.
- IPCC (2005), *Special Report on Carbon Dioxide Capture and Storage*, edited by B. Metz et al., Cambridge Univ. Press, Cambridge, U. K.
- Kandhai, D., D. Hlushkou, A. G. Hoekstra, P. M. A. Sloot, H. V. As, and U. Tallarek (2002), Influence of stagnant zones on transient and asymptotic dispersion in macroscopically homogeneous porous media, *Phys. Rev. Lett.*, *88*, 234501.
- Kang, P. K., M. Dentz, T. Le Borgne, and R. Juanes (2011), Spatial Markov model of anomalous transport through random lattice networks, *Phys. Rev. Lett.*, *107*, 180602.
- Le Borgne, T., and P. Gouze (2008), Non-Fickian dispersion in porous media: 2. Model validation from measurements at different scales, *Water Resour. Res.*, *44*, W06427, doi:10.1029/2007WR006279.
- Le Borgne, T., M. Dentz, and J. Carrera (2008), Lagrangian statistical model for transport in highly heterogeneous velocity fields, *Phys. Rev. Lett.*, *101*, 090601.
- Mordant, N., J. Delour, E. Lèveque, A. Arnéodo, and J.-F. Pinton (2002), Long time correlations in Lagrangian dynamics: A key to intermittency in turbulence, *Phys. Rev. Lett.*, *89*(25), 254502.
- Moroni, M., N. Kleinfelder, and J. H. Cushman (2007), Analysis of dispersion in porous media via matched-index particle tracking velocimetry experiments, *Adv. Water Res.*, *30*(1), 1–15.
- Mostaghimi, P., B. Bijeljic, and M. J. Blunt (2012), Simulation of flow and dispersion on pore-space images, *SPE J.*, *17*, 1131–1141.
- OpenFOAM (2011), The open source CFD toolbox. [Available at <http://www.openfoam.com>.]
- Orr, F. M. Jr., and J. J. Taber (1984), Use of carbon dioxide in enhanced oil recovery, *Science*, *224*, 563–569.
- Pope, S. B. (2000), *Turbulent Flows*, 8th ed., Cambridge Univ. Press, Cambridge, U. K.
- Risken, H. (1989), *The Fokker–Planck Equation*, 2nd ed., Springer, Berlin, Germany.
- Rolle, M., D. Hochstetler, G. Chiogna, P. K. Kitanidis, and P. Grathwohl (2012), Experimental investigation and pore-scale modeling interpretation of compound-specific transverse dispersion in porous media, *Transp. Porous Media*, *93*(3), 347–362.
- Scheven, U. M., D. Verganelakis, R. Harris, M. L. Johns, and L. F. Gladden (2005), Quantitative nuclear magnetic resonance measurements of preasymptotic dispersion in flow through porous media, *Phys. Fluids*, *17*, 117107.
- Szulcowski, M. L., C. W. MacMinn, H. J. Herzog, and R. Juanes (2012), Lifetime of carbon capture and storage as a climate-change mitigation technology, *Proc. Natl. Acad. Sci. U.S.A.*, *109*(14), 5185–5189.
- Tartakovsky, A. M. (2010), Langevin model for reactive transport in porous media, *Phys. Rev. E*, *82*, 026302.
- Tartakovsky, A. M., G. Redden, P. C. Lichtner, T. D. Scheibe, and P. Meakin (2008), Mixing-induced precipitation: Experimental study and multiscale numerical analysis, *Water Resour. Res.*, *44*, W06S04, doi:10.1029/2006WR005725.
- Taylor, G. I. (1921), Diffusion by continuous movements, *Proc. London Math. Soc.*, *20*, 196–211.
- Tejedor, V., and R. Metzler (2010), Anomalous diffusion in correlated continuous time random walks, *J. Phys. A: Math. Theor.*, *43*(8), 082002.
- Willingham, T. W., C. J. Werth, and A. J. Valocchi (2008), Evaluation of the effects of porous media structure on mixing-controlled reactions using pore-scale modeling and micromodel experiments, *Environ. Sci. Technol.*, *42*, 3185–3193.
- Yoshida, N., and Y. Takahashi (2012), Land-surface contamination by radionuclides from the Fukushima Daiichi Nuclear Power Plant accident, *Elements*, *8*(3), 201–206.